

OPEN ACCESS

Effect of microstructure of nano- and micro-particle filled polymer composites on their tribo-mechanical performance

To cite this article: D Devaprakasam *et al* 2008 *J. Phys.: Conf. Ser.* **126** 012057

View the [article online](#) for updates and enhancements.

Related content

- [Deflection and Buckling behaviour of simply supported nanocomposite beams under FSDT approach](#)
P Pramod kumar, V V Subbarao, S Sarath Chandra *et al.*
- [A review on Diels-Alder based self-healing polymer composites](#)
N I Khan, S Halder, S B Gunjan *et al.*
- [Dielectric studies on PEG-LTMS based polymer composites](#)
Ravikumar V Patil, D Praveen and R Damle

Recent citations

- [Physical Characterization of Bismuth Oxide Nanoparticle Based Ceramic Composite for Future Biomedical Application](#)
Pravin Jagdale *et al*
- [The Impact of Selected Atmospheric Conditions on the Process of Abrasive Wear of CFRP](#)
Aneta Krzyzak *et al*
- [The Mechanical and Physical Properties of 3D-Printed Materials Composed of ABS-ZnO Nanocomposites and ABS-ZnO Microcomposites](#)
Nectarios Vidakis *et al*



ECS **240th ECS Meeting**
Oct 10-14, 2021, Orlando, Florida

Register early and save up to 20% on registration costs

Early registration deadline Sep 13

REGISTER NOW

Effect of microstructure of nano- and micro-particle filled polymer composites on their tribo-mechanical performance.

D. Devaprakasam¹, P.V. Hatton², G. Möbus¹ and B.J. Inkson¹.

¹Department of Engineering Materials, University of Sheffield, UK.

² Centre for Biomaterials and Tissue Engineering & Department of Clinical Dentistry, University of Sheffield, UK

E-mail: D.Deivasagayam@sheffield.ac.uk

Abstract. In this work we have investigated the influence of nanoscale and microscale structure on the tribo-mechanical performance and failure mechanisms of two biocompatible dental polymer composites, with different reinforcing particulates, using advanced microscopy techniques. Nano- and microstructural analysis reveals the shape, size and distribution of the particles in the composites. In the microparticle filled polymer composite (microcomposite), the particles are of irregular shape with sharp edges with non-uniform distribution in the matrix. However, in the nanoparticle filled composites (nanocomposite), filler particles are spherical in shape with uniform distribution in the matrix. From nanoindentation measurements, hardness and reduced modulus of the microcomposite were found to be heterogeneous. However, the hardness and reduced modulus of the nanocomposite were found to be homogeneous. The nanocomposite shows better tribo-mechanical performance compared to that of the microcomposite.

1. Introduction

Nanoscale interactions have profound implications on the macroscopic behaviour of materials as every structural level contributes to the mechanical stability and durability of the resulting materials. It has become increasingly important to understand and manipulate materials at the nanoscale to develop new functional materials for engineering and biomedical applications. Nanostructured and nanocomposite [1] materials can show dramatic improvement of mechanical, tribological, electrical and chemical properties. New materials used for biomedical applications, including bio-implants, restorations and replacements require matching mechanical properties, high durability and biocompatibility. Restorative materials used in dental applications require long term durability. In dental restorative applications, nanoparticle reinforced polymer composite materials [1-3] have attracted huge interest in recent years, due to many advantages over traditionally used microparticle reinforced polymer composites. Nanoparticles used as filler in the polymer composites can be dispersed uniformly and lead to high fracture toughness compared to microparticle reinforced polymer composites [4]. In this work we addressed the structure-properties relation of the microcomposite and the nanocomposite on the tribo-mechanical performance at the nanoscale.

2. Materials and Methods

The microcomposite is a mixture of silica (SiO_2) microparticles and a resin matrix based on various monomeric dimethacrylates Bis-GMA, TEGDMA, UDMA, which is called EsthetX, obtained from Dentsply, USA. The nanocomposite is a mixture of zirconia (ZrO_2)/ silica (SiO_2) nanoparticles, nanoclusters of nanoparticles, and the same resin matrix, which is called Filtek Supreme Standard, obtained from 3M ESPE, USA. For transmission electron microscope (TEM) analysis, 100 nm thick samples were cut with a diamond knife using the ultramicrotomy procedure and samples were collected on the gold coated copper TEM mesh. For atomic force microscope (AFM) and lateral force microscope (LFM) measurements 10 mm diameter and 1 mm thick discs of the nanocomposite and microcomposite were prepared on freshly cleaved mica sheets using the visible light curing technique at room temperature. A Philips EM420 was used for the TEM analysis. AFM and LFM measurements were carried out using a Nanoscope IIIa AFM with DNP-20 V-shaped silicon nitride cantilever probe of stiffness 0.06 N/m with tip radius of $\sim 30\text{nm}$. Tapping mode measurements were carried out using a rectangular phosphorous doped silicon cantilever (MPP-11100) of stiffness 40 N/m with nominal tip radius $\sim 10\text{nm}$ and resonant frequency of 364 kHz. Nanowear measurements were carried out using a rectangular stainless steel cantilever (PDNISP) of stiffness 240N/m with diamond tip of radius $\sim 40\text{nm}$. Nanoindentation measurements were carried out using a Hysitron nanoindenter with Berkovich diamond indenter of tip radius $\sim 150\text{nm}$.

3. Results

3.1. Nano/Microstructure characterization

Figures 1a and 1b show a tapping mode phase image and a TEM image of the microcomposite. The measured surface roughness (σ_{rms}) of the microcomposite is about 50 nm. The primary particles in the microcomposite (figure 1a) have a bimodal size distribution ranging from 100 nm to 500nm and 1 μm to 4 μm , irregular shapes with sharp edges and non uniform distribution of the particles. Figure 1c and 1d show friction and TEM images of the nanocomposite. The nanoparticles are uniformly distributed in the resin matrix, the size of the nanoparticles is about 60 nm and the measured surface roughness (σ_{rms}) is about 20 nm.

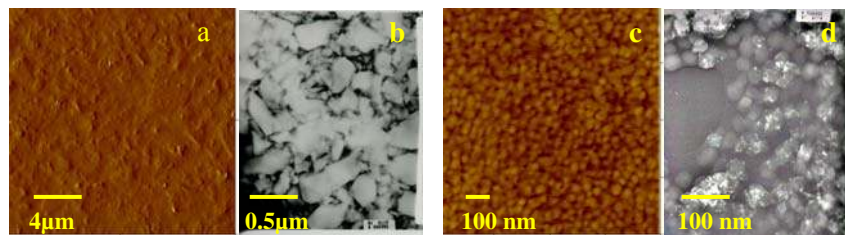


Figure 1. (a) AFM tapping mode phase image and (b) TEM image of the microcomposite, the particle sizes vary from 100 nm to 4 μm ; (c) LFM image and (d) TEM image of nanocomposite, the nanoparticle sizes vary from 40-60nm

3.2. Nanomechanical properties (Modulus (E_r), Hardness (H))

Figures 2a and 2b show load-displacement curves of the microcomposite and nanocomposite respectively for a maximum applied load of P_{max} , $\sim 425\mu\text{N}$. For the microcomposite the contact stiffness (i.e slope of the unloading part of the load-displacement curve) varies for a given maximum applied load due to heterogeneous mechanical properties. However, for the nanocomposite the deviation in the contact stiffness is minimal due to homogeneous mechanical properties. Nanoindentation on high packing density areas of the microcomposite results in high contact stiffness, modulus and hardness but nanoindentation on polymer or low packing density areas of the microcomposite yields low contact stiffness, modulus and hardness. Hardness and reduced modulus of the microcomposite measurements vary widely but for the nanocomposite the variations are minimal.

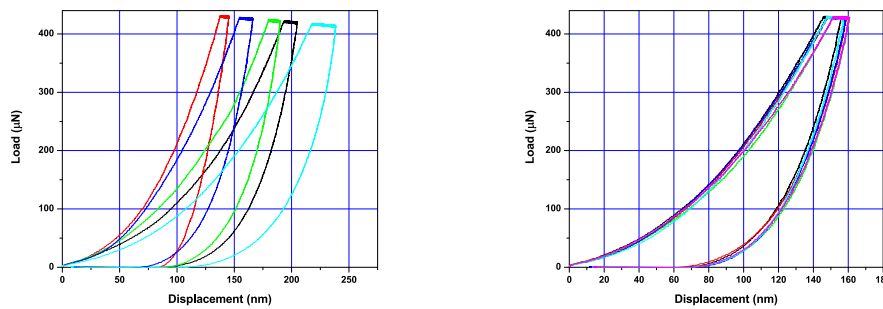


Figure 2. Nanoindentation characterisation: (a) force-displacement curves of the microcomposite with maximum applied load, P_{max} , $\sim 425\mu\text{N}$ and (b) force-displacement curves of the nanocomposite with maximum applied load, P_{max} , $\sim 425\mu\text{N}$

For the microcomposite the hardness (H) varies from 0.4 GPa to 1.7 GPa and the reduced modulus (E_r) varies from 8 GPa to 22 GPa. For the nanocomposite the hardness (H) varies from 0.75 GPa to 1.15 GPa and the reduced modulus (E_r) varies from 13.5 to 19 GPa.

3.3. Nanotribological properties (friction, wear)

Friction measurements were carried out in LFM mode, the friction force being measured by averaging the friction force images for the same scan area $1\mu\text{m} \times 1\mu\text{m}$ [5-7]. Figure 3a shows friction force versus applied load. Friction forces of the microcomposite are always greater than for the nanocomposite for a given applied load and a steep increase of the friction force at higher applied load was observed for the microcomposite.

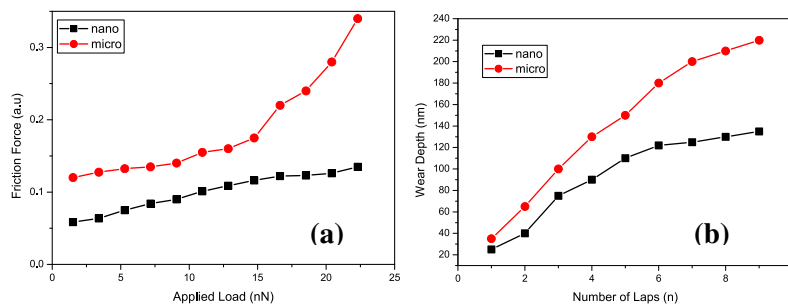


Figure 3. (a) Friction force versus the applied load of the microcomposite (filled circle) and the nanocomposite (filled square). (b) The wear depth (nm) versus the number of scanning laps (n) of the microcomposite (filled circle) and the nanocomposite (filled square).

Figure 3b shows measured wear depth versus number of scanning laps for the applied load of $\sim 15\mu\text{N}$ and the scan area of $10\mu\text{m} \times 10\mu\text{m}$. The wear depth of both the microcomposite and the nanocomposite increases with scanning lap and the microcomposite shows a higher wear rate than the nanocomposite.

3.4. Failure mechanisms (nanoscratch, nano-/micro-wear, nanofracture)

SEM examination of the wear crater figures 4a-d reveal different failure mechanisms of the microcomposite and nanocomposite. In the microcomposite, large particles get removed due to weak bonding and delamination between the particles and matrix interface. The crater created by the removal of a large particle which acts as a hot spot for wear. Subsequent scan laps around the crater leads to rapid removal of material resulting in high wear.

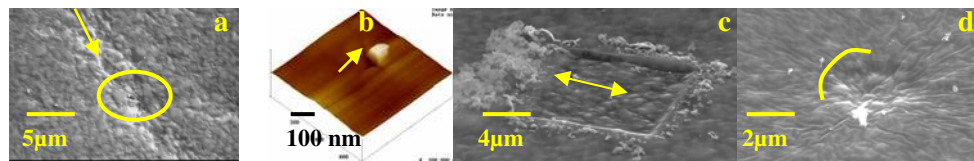


Figure 4 a-d show failure mechanisms of the microcomposite and nanocomposite: (a) a wear scar on the microcomposite due to a scratch (an arrow indicates the scratch direction and the circle indicates the crater) (b) AFM scan of lateral movement (along arrow direction) of a filler particle in the microcomposite; (c) worn area and associated debris of the nanocomposite (arrow indicates the scratch direction) and (d) micro-crack on the nanocomposite, the fracture initiated by indentation.

4. Discussion

Nanoscale and microscale structure measurements show a bimodal distribution of filler particles in the microcomposite which have irregular shapes, sharp edges and heterogeneous distribution in the matrix. Nanoindentations show a wide variation in the elastic modulus ($E \approx E_r$), 8-22 GPa and the hardness (H), 0.5-1.7 GPa. The high and low values of the measured elastic modulus (E) and hardness (H) of the microcomposite correspond to the regions with high and low particle packing density respectively. During sliding contact, the sharp edges of particles increase the friction, heterogeneous mechanical properties result in high energy dissipation and big particles with weak interfacial bonding get removed resulting in big craters on the sliding surface which act as failure hot-spots. Failure mechanisms of the microcomposite were dominated by large particle removal due to indentation and scratch. In the case of nanocomposites, the nanoparticles have spherical shape, uniform distribution and relatively strong interfacial bonding between the particles and the matrix. Uniform packing density of nanoparticles in the polymer matrix results in homogeneous mechanical properties. The measured values of the elastic modulus ($E \approx E_r$), 13.5 -19 GPa, and the hardness (H), 0.75-1.15 GPa, are in a very narrow range. During sliding, the spherical nanoparticles act as bearings which lead to low frictional resistance to the AFM probe, failure mechanisms are dominated by gradual removal of nanoparticles and polymer matrix. The strong interfacial bonding between the nanoparticles and the matrix due to high specific surface area of nanoparticles enhances the wear resistance of the nanocomposite which results in better nanotribological performance compared to that of the microcomposite.

Acknowledgments

The authors are grateful to EPSRC, UK, for financial support (GR/S85689/01).

References

- [1] Komarneni S 1992 *J. Mater. Chem.* **2** (12) 1219-1230.
- [2] Hengh L 1991 *J. Am. Ceram. Soc.* **74** (7) 1487-1510.
- [3] Mitra S B, Dong Wu, Holmes B N 2003 *J. Am. Dent. Assoc.* **134** 1382-1390.
- [4] Bushan B, 2001, *Modern Tribology Handbook: Vol. I and II*, CRC Press, Washington, USA.
- [5] Oliver W C, Pharr G M 2004 *J. Mater. Res.* **9**(1) 3-20.
- [6] Devaprakasam D, Khatri O P, Shankar N, Biswas S K 2005 *Tribology International* **38** 1022-1034.
- [7] Carpick R W 1997 *Chem. Rev.* **97** 1163-1194.